Journal of
Water, Sanitation & Hygiene for Development

IWA PUBLISHING

 Journal of Water, Sanitation and Hygiene for Development Vol 14 No 10, 988 doi: 10.2166/washdev.2024.206

Research Paper

Adsorption dynamics of chloride removal with activated vetiver root powder: dynamic modeling perspectives and ANN predictions

Riddhi Chandrakant Dhumal [a,*] and Parag Sadgir [b]

[a] Civil Engineering Department, College of Engineering, Pune, India
[b] Civil Engineering Department, COEP Technological University, Pune India
*Corresponding author. E-mail: rcd21.civil@coeptech.ac.in

RCD, 0000-0001-8710-6593

ABSTRACT

This study evaluates activated vetiver root powder as chloride ion adsorbent for saline water treatment. Experimental results demonstrate that activated vetiver root effectively removes chloride ions from saline solutions. Higher bed heights and lower flow rates improve efficiency by providing more adsorption sites and a longer contact time. However, higher concentrations lead to rapid bed exhaustion, highlighting the need for parameter optimization. Dynamic adsorption modeling using Thomas, Yoon–Nelson, and Clark models assesses the impact of bed height, flow rates, and initial concentration on chloride removal efficiency. Breakthrough equations closely fitted experimental data in the following order: Thomas model ($R^2 = 0.999$) > Clark ($R^2 = 0.996$) > Yoon–Nelson ($R^2 = 0.994$). Scanning electron microscopy (SEM) analysis identifies pores and pockets as main surface components. Insights into adsorption mechanisms were gained through infrared and X-ray spectroscopies. A novel predictive algorithm for chloride removal in a continuous mode was developed using neural networks. Artificial neural network (ANN) prediction ability was assessed using MSE and R^2 values. Future commercial applications of activated vetiver powder can be investigated using real salinity-induced wastewater. Additionally, assessing the adsorbent's regeneration and reusability is vital for confirming its cost-effectiveness and sustainability in longstanding use. This study offers perceptions for developing efficient water treatment strategies by understanding adsorption dynamics and surface characteristics for optimizing chloride removal processes.

Key words: activated vetiver root powder, breakthrough, chloride ion removal, dynamic adsorption modeling, parameter optimization

HIGHLIGHTS

- Evaluation of activated vetiver root powder for chloride ion adsorption in the column study.
- Insights into dynamic modeling using both linear and non-linear approaches for chloride removal.
- Impact of key parameters (bed height, flow rates, initial concentration) on adsorption efficiency.
- Superior fit of the Thomas model for chloride adsorption dynamics.

GRAPHICAL ABSTRACT

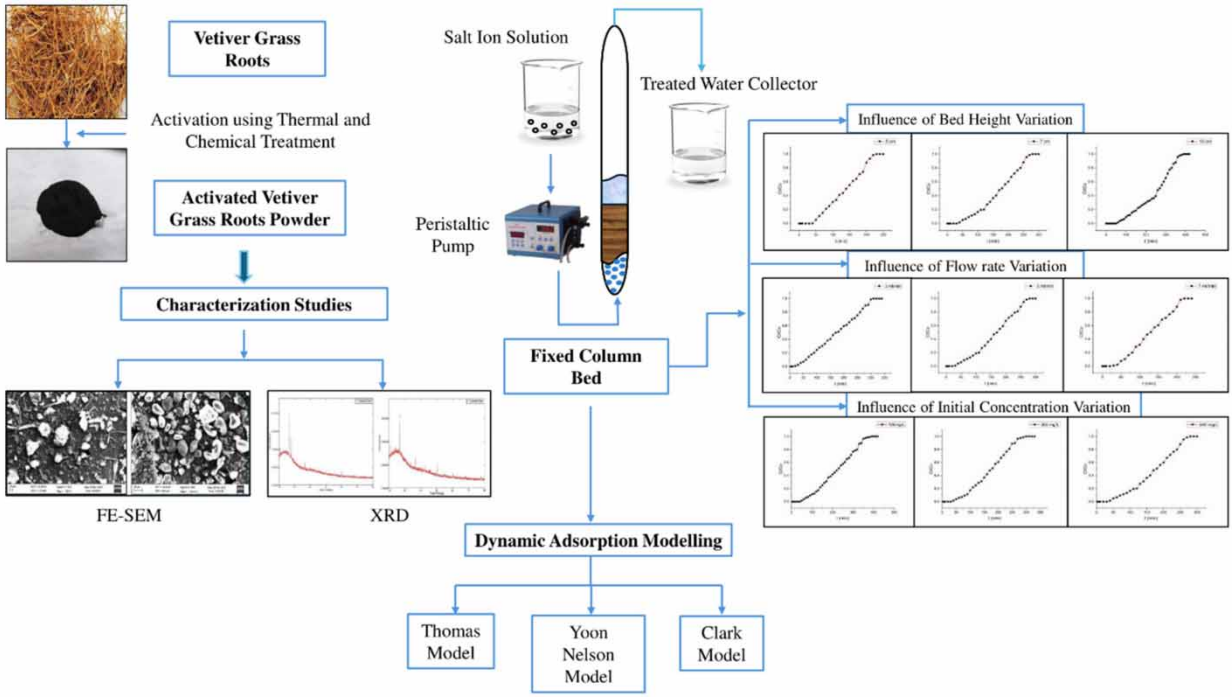

INTRODUCTION

Chloride contamination is a formidable challenge to environmental sustainability and public welfare worldwide (Sharma & Bhattacharya 2017). With origins spanning industrial discharge, agricultural runoff, and road de-icing practices, elevated chloride levels present a pervasive threat. Their infiltration into freshwater ecosystems induces salinization, disrupting delicate ecological balances and endangering aquatic life (Dey *et al.* 2024).

Saline water, often a source of chloride contamination, unveils issues in the agriculture environments wherein irrigated water needs regular monitoring. Nevertheless, not much investigation caters to alleviating water salinity for the purpose of irrigation (Kaushal *et al.* 2021). A high concentration of chloride in irrigation water can inhibit crop development and degrade soil quality, demonstrating the necessity for efficient chloride removal processes in water treatment (Johnson *et al.* 1989; Karaivazoglou *et al.* 2005).

Reverse osmosis (RO) and other desalination technologies have the potential to address water salinity challenges but possess significant limitations due to high capital and operating costs among many others (Hoek *et al.* 2022). These limitations prompt the research into exploring low-cost alternative treatments using organic compounds.

The recent upsurge of interest in natural adsorbents for specific ion removal is driven by their abundance, cost-effectiveness, and ecological sustainability (Dhumal & Sadgir 2023). Activated carbon, which consists of amorphous carbonaceous substances exhibiting elevated porosity and internal surface area (Fierro *et al.* 2008), is a key component in this study. Among these, activated vetiver root powder stands out as a promising candidate for chloride ion adsorption due to its substantial physical and chemical properties. Vetiver is harvested throughout numerous tropical and subtropical countries, encompassing India, Indonesia, Madagascar, etc. The production serves multiple purposes, including antimicrobial and antioxidant properties. Furthermore, vetiver roots perform a substantial part in soil conservation and assist with stabilizing the dikes (Altenor *et al.* 2013).

This article examines the use of activated vetiver root powder as a bioadsorbent for continuous removal of chloride ions in water treatment. By employing dynamic adsorption modeling with Thomas, Yoon–Nelson, and Clark models, it investigates the effects of bed height, flow rate, and initial concentration on chloride removal efficiency. The activated adsorbent's surface properties and adsorption mechanisms are also examined in this work. Additionally, it introduces a predictive artificial neural network (ANN) for chloride ion removal efficiency in continuous mode. Furthermore, this study provides invaluable

comprehensions on strengthening the design and functioning of adsorption-based water treatment systems, advocating sustainable practices for the foreseeable future.

MATERIALS AND METHODS

Material preparation

The materials for adsorption were carefully prepared to ensure optimal performance. Initially, the adsorbent underwent thorough cleaning with tap water followed by rinsing with deionized water to eliminate dust, dirt, and impurities. After cleaning, the vetiver roots were dried at 105 °C for 5 h, ground into powder, and sieved to achieve uniform particle size.

Vetiver root powder underwent activation by heating to 600 °C and applying phosphoric acid (1:4 ratio (M/V)). The outcome of this thermal and chemical treatment is the activated powder which was stored for subsequent use (Harikumar *et al.* 2010).

For the adsorbate preparation, a 500-ppm NaCl solution was meticulously formulated by dissolving anhydrous sodium chloride in deionized water. pH adjustments were made using 0.1 M NaOH or HCl solutions. All chemicals were of analytical grade, sourced locally from Maharashtra, India.

Characterization of adsorbent

The surface morphology and microstructure of the adsorbent were examined using scanning electron microscopy (SEM). By utilizing SEM, high-resolution images were obtained, which unveiled the surface texture, porosity, and structural characteristics of the adsorbent material. These images were instrumental in pinpointing any irregularities, cracks, or pores, providing valuable insight into the adsorption capabilities and interaction mechanisms between the activated adsorbent and Cl^- ions.

The physicochemical properties of vetiver biomass were comprehensively analyzed to understand its intrinsic characteristics and potential interactions with metal ions. To elucidate detailed information about the crystallographic structure of the biomass and its structural features, X-ray diffraction (XRD) was utilized. The biomass was analyzed using Cu Kα radiation, and the scan angle ranged from 20° to 80° at a speed of 2° per minute.

Continuous column system

The adsorption of Cl^- ions on activated vetiver root powder was analyzed by employing the continuous column method, following the methodology as illustrated in Figure 1.

The experiments were carried out in a glass column with a diameter $D = 2$ cm and height $H = 48$ cm. The bed comprised activated vetiver root powder with an average particle diameter of 3.4 nm. It was secured in place with the help of glass wool below and above the bed to avoid expansion of the column bed. The adsorbate feed solution of chloride ions was fed from the bottom of the column as shown in the schematic with the help of a peristaltic pump. Column outputs were collected from the top of the column at regular intervals as illustrated in Figure 2. The concentration of chloride ions in aqueous solutions was determined with the help of Ion Chromatography (Metrohm-Eco IC).

Adsorption dynamics

The overall chloride ion adsorption capacity for a specific initial adsorbate concentration and rate of flow corresponds to the integral of the plot depicting the concentration of adsorbed ions against the effluent time.

The total adsorbed Cl^- ion quantity or the maximum of column capacity (q_{total}), in mg, for a given feed concentration and flow rate (Maleki *et al.* 2020), is provided in the following (Equation (1)):

$$q_{\text{total}} = Q \cdot A \cdot C_o/1,000 = \frac{Q}{1,000}\int_{t=0}^{t=t\text{total}} C(t)\,\mathrm{d}t = q_e \cdot m \tag{1}$$

Here, t_{total} represents the overall flow duration in minutes, Q symbolizes the flow rate in ml/min, A denotes the total area beneath the breakthrough curve, Co is the initial concentration of the adsorbate and qe (mg/g) is the column adsorption capacity.

The theoretical total of Cl^- ions adsorbed by the column is determined by the Equation (2)

$$m_{\text{total}} = \frac{(C_o \times Q \times t_{\text{total}})}{1,000} \tag{2}$$

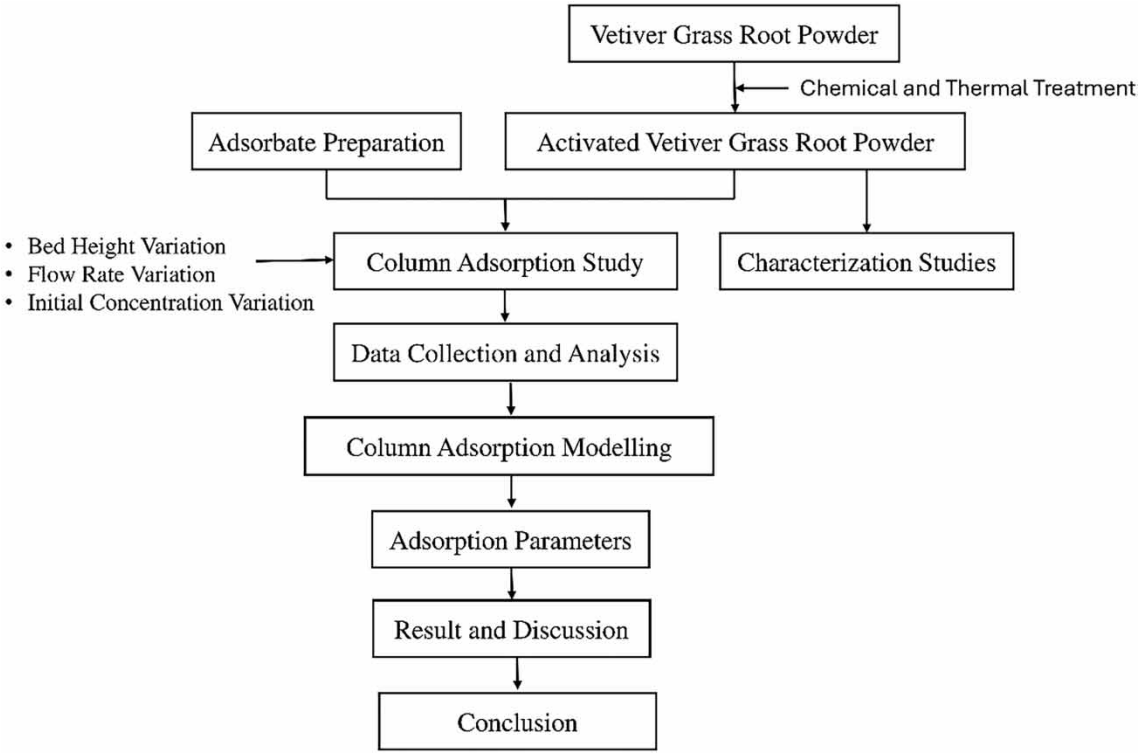

Figure 1 | Flowchart for column adsorption methodology.

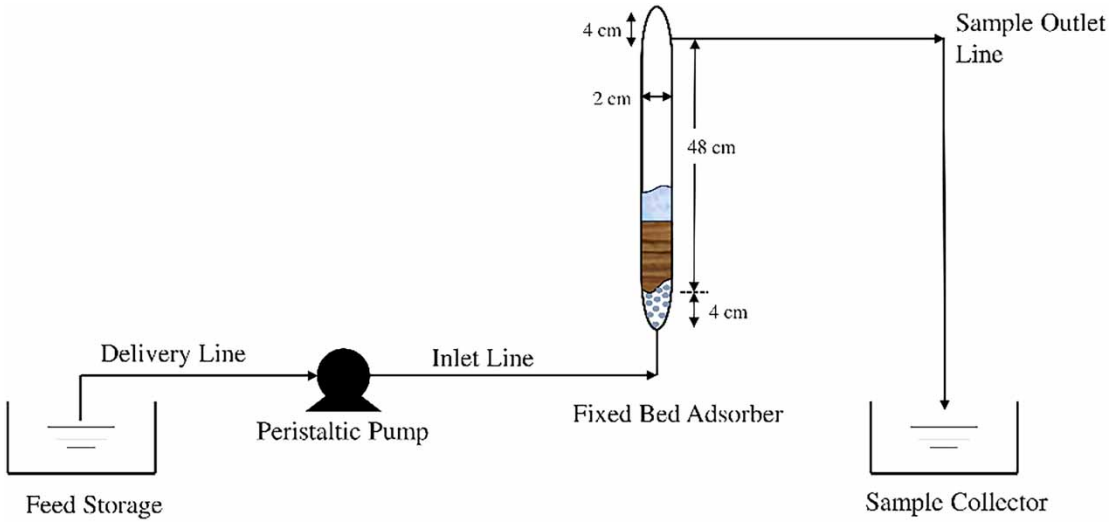

Figure 2 | Column schematic.

With knowledge of the total mass of adsorbed ions and the overall sorbent capacity, one can compute the total percentage of Cl^- ions removed using Equation (3)

$$\%Cl^- \text{ ions removed} = \left(\frac{q_{total}}{m_{total}}\right) \times 100\% \quad (3)$$

Synthetic chloride solutions were used in column adsorption tests. The investigations were carried out by choosing experimental settings until the activated adsorbent attained exhaustion with different bed heights (5, 7, and 10 cm), flow rates (3, 5, and 7 ml/min), and initial chloride concentrations (100, 300, and 500 mg/l). The study intends to offer an extensive comprehension of the chloride bioadsorption process based on varying operational parameters, which is crucial for optimizing practical applications for water treatment.

Uncertainties inherent in the experimental measurements were incorporated in the study with error propagation analysis. The flow rate was controlled at 3, 5, and 7 ml/min each with an uncertainty of ± 0.5 ml/min. The initial chloride concentration was 100, 300, and 500 mg/l with an uncertainty of ± 50 mg/l. The bed height was measured at 5, 7, and 10 cm with an uncertainty of ± 0.5 cm. To obtain error estimates for derived values like the total adsorbed amount (qtotal), the total mass of chloride removed (mtotal), and the adsorption capacity (q_e), these uncertainties were propagated through the calculations. The results are illustrated in Table 2.

A multitude of models, including the Thomas, Yoon–Nelson, and Clark models, are utilized to anticipate the dynamic behavior of the column. This predictive capability is vital for accurately forecasting the breakthrough curve of effluent parameters, ultimately ensuring the productive design and optimization of a column adsorption process.

Column adsorption modeling

In adsorption studies, understanding the process dynamics is crucial for optimization. Breakthrough curves, which depict concentration changes over time, are key tools for visualizing the saturation process within adsorbent materials (Hu *et al.* 2022). Steeper curves suggest more effective adsorption. Various adsorption dynamics models predict these curves and provide insights into adsorbent behavior, determining key parameters like kinetic coefficients and maximum adsorbent capacity (Chu 2004). The Levenberg–Marquardt method, implemented via Origin 9 software, is used to infer these parameters.

Table 1 summarizes column models used to study chloride ion adsorption on activated adsorbent. The Thomas model, widely used in column performance theory, has its equation included with K_{Th} (ml/min/mg) as the rate constant and q_{o} (mg/g) as the maximum solid-phase solute concentration. The Thomas model is prominently used because of its simplicity, precision in comprehending and consistent results that are dependable in predicting breakthrough curves, assuming a plug flow behavior of the adsorbate through the bed. In the Thomas model, adsorption is assumed to be governed by second-order reaction kinetics, and it is also assumed that the rate of adsorption is not restricted by external mass transfer (Benjelloun *et al.* 2021).

The Yoon and Nelson model for a single-component system includes $K_{\mathrm{Y-N}}$ (1/min) as the rate constant, τ (min) as the time for 50% breakthrough, and t (min) as the breakthrough time. These parameters are derived from experimental data to compute theoretical breakthrough curves. The rate constants involved in the adsorption process are predicted using time-based data. The Yoon–Nelson model does not put emphasis upon the nature of the adsorbent or properties of adsorbate (Djelloul & Hamdaoui 2015). Experimental characteristics such as flow rate and initial concentration have a major impact on the accuracy of the model (Darweesh & Ahmed 2017).

Clark's model, which integrates mass transfer concepts with the Freundlich isotherm, includes parameters A and r for the kinetic equation and n as the Freundlich isotherm exponent. The Clark model's capability to represent adsorption kinetics and equilibrium scenarios is significant, such as on heterogeneous adsorbent surfaces or in distinct pore structures. Studies have shown that within these complex systems, the Clark model effectively forecasts breakthrough curves (Hu *et al.* 2020).

Table 1 | Fixed-bed column adsorption models

Model	Non-linear equation	Plot	Model parameters
Thomas	$\frac{C_t}{C_0} = \frac{1}{1 + e^{[k(q_0 \cdot m/Q) - (C_0 \cdot t)]}}$	$\frac{C_t}{C_0}$ vs. t	K_{Th} and q_e
Yoon-Nelson	$\frac{C_t}{C_0} = \frac{1}{1 + e^{k(t-1)}}$	$\frac{C_t}{C_0}$ vs. t	$K_{\mathrm{Y-N}}$ and τ
Clark	$\frac{C_t}{C_0} = \frac{1}{(1 + A_C \cdot e^{-rt})^{\frac{1}{n-1}}}$	$\frac{C_t}{C_0}$ vs. t	A and r

Computation modeling

ANNs have been employed for modeling of various ion removals using bioadsorbents (Khandanlou *et al.* 2016; Fawzy *et al.* 2018). Similarly, ANN studies in continuous column mode were reported to show accuracy for predictive modeling (Yetilmezsoy & Demirel 2008). The ANN model was created to mimic the adsorption process and predict the adsorption capacities (q_e) using input factors like initial concentration, flow rate, contact time, % of chloride removed, q_{total}, m_{total}, and volume of treated saline water at the breakthrough and saturation points as shown in Table 4 (Das & Mishra 2021). The ANN model was constructed using a multi-layer perceptron (MLP) architecture. It included an input layer corresponding to the number of input variables, hidden layers, and an output layer representing the predicted adsorption performance. Rectified Linear Unit (ReLU) activation functions were used for the hidden layers and a linear activation function for the output layer (Yusuf *et al.* 2020). The Levenberg–Marquardt algorithm was used for network training. The metrics used for analyzing the robustness and reliability ANN model included R^2 values and RMSE values (Parsaei *et al.* 2022).

RESULTS AND DISCUSSIONS

Characterization of adsorbent

Figure 3 shows the surface characteristics of vetiver root powder prior to and following activation. In the beginning, the surface emerged smooth and dense, with no porous formations. SEM identified the lack of homogeneity in the size of particles and shape. Activated vetiver root powder exhibited an inconsistent texture and clearly defined pore structure after treatment. Phosphoric acid activation significantly affected the development of pore spaces on substrates.

XRD exploration of vetiver root powder (Figure 4) uncovers contrasting characteristics before and after activation. Initially, the spectrum displays projecting diffraction peaks, signaling a chiefly crystalline configuration, remarkably centered at 2θ values of 20.85° and roughly 26.70°, suggesting an enhanced regularity in the crystalline configuration. In-depth XRD analysis, Brunauer–Emmett–Teller (BET) and Fourier Transform Infrared analysis (FTIR) of the vetiver root powder used in this study was previously conducted and reported in detail in (Dhumal & Sadgir 2024).

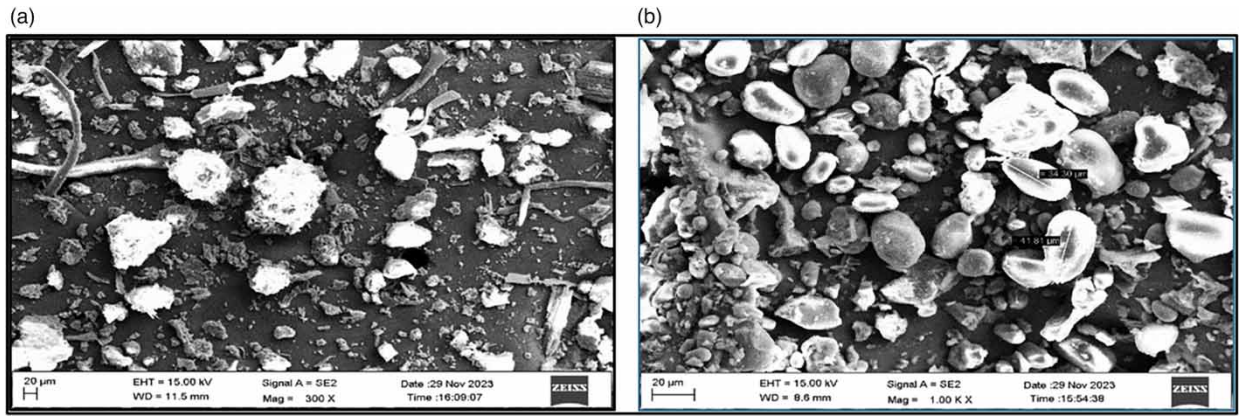

Figure 3 | SEM analysis of the vetiver powder before (a) and after activation (b).

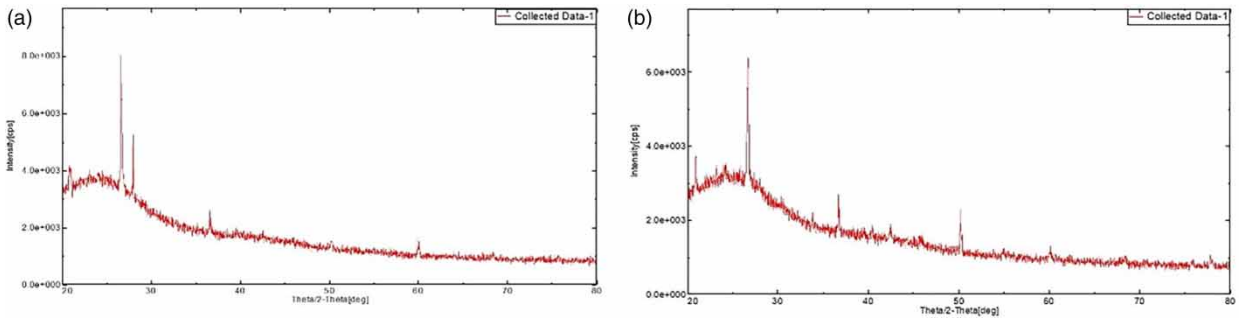

Figure 4 | XRD images of the vetiver powder before (a) and after activation (b).

Column-operating parameters

Effect of the column bed height

The effect of the bed height on column performance is demonstrated by the saturation times observed in the breakthrough curves (Figure 5). It was observed that with the increase in the height of the bed from 5 to 7 cm and further to 10 cm, the saturation time also increased from 220 to 270 min and then to 380 min, respectively. This occurrence may be ascribed to the heightened surface area and the augmented quantity of binding sites accessible for adsorption with the elevation of the bed height (Patel 2019).

The increase in bed height for chloride ion removal results in a greater number of accessible sites for adsorption and an extended contact time involving the chloride ions and the adsorbent material. This leads to higher removal efficiency of chloride ions from the saline solution (Han *et al.* 2009; Ahmad & Hameed 2010). Higher bed columns exhibit improved performance, as reported in previous literature (Omitola *et al.* 2022).

Moreover, the slower exhaustion of the adsorbent bed is desirable for the effective removal of chloride ions from the saline solution. Therefore, higher bed heights are preferable for the operation, as they provide a longer duration of effective adsorption (Mondal 2009). This implies that water treatment plants can enhance their column designs by using taller adsorption beds, leading to substantial improvements in the removal of contaminants from water (Al-dhawi *et al.* 2024).

Effect of the flow rate

The impact of altering the volumetric flow rate was explored across different rates of chloride ion flow. Breakthrough curves were derived under flow rates of 3, 5, and 7 ml/min, with consistent initial concentration (500 mg/l) and bed height (7 cm, considering the % removal rate of chloride in 7 and 10 cm bed height is almost similar), as illustrated in Figure 6. It was observed that the time required to reach saturation increased as the flow rate decreased. For instance, the saturation time increased from 210 min at 7 ml/min to 270 min at 5 ml/min and eventually to 300 min at 3 ml/min.

A corresponding enhancement in removal efficiency was observed with the decrease in flow rate, indicating that lower flow rates are more suitable for the adsorption process. This is attributed to the fact that at lower flow rates, chloride ions are afforded additional time to permeate into the pores of the adsorbent substance, allowing for better utilization of the available binding sites and achieving adsorption equilibrium.

Conversely, at higher flow rates, chloride ions have less residence time in the column, resulting in incomplete utilization of the adsorbent material's capacity and potentially leading to desorption of previously adsorbed ions. This rapid passage of chloride ions through the column results in earlier breakthrough times and higher concentrations of chloride ions in the effluent.

Therefore, low flow rates are beneficial for chloride ion removal in fixed-bed columns due to their higher adsorption capacity, as observed in similar studies (Han *et al.* 2009; Albadarin *et al.* 2012). However, in real-world water treatment environments, it is essential to regulate the flow rate to ensure effective removal of contaminants. Slower flow rates can improve adsorption but may decrease the volume of treated water per time unit (Abdiyev *et al.* 2023).

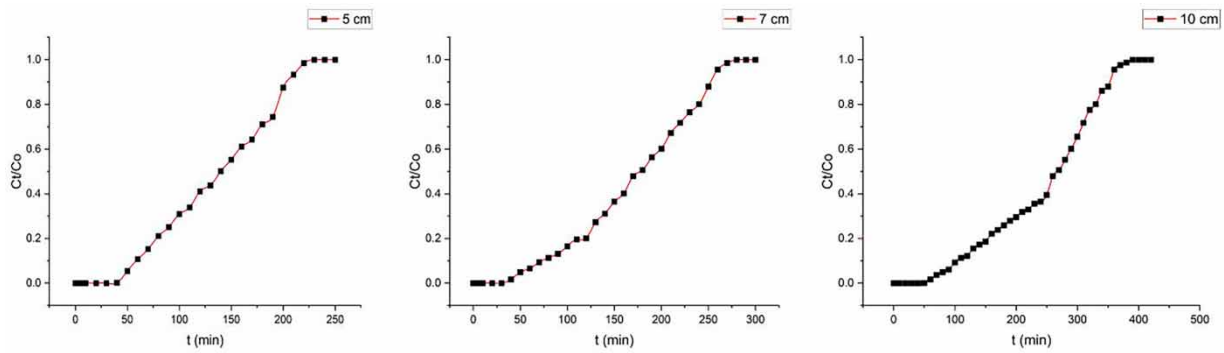

Figure 5 | Effect of a column-operating parameter – bed height on the breakthrough curve.

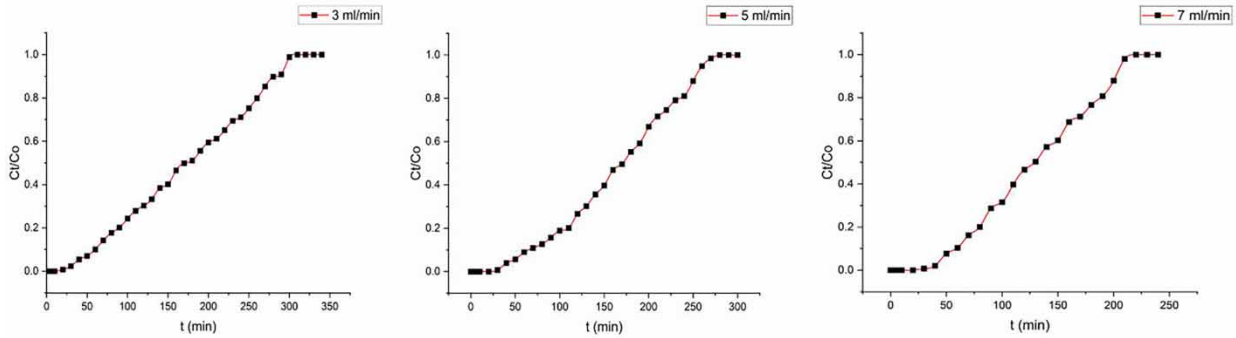

Figure 6 | Effect of a column-operating parameter – flow rate on the breakthrough curve.

Effect of the initial concentration of adsorbate

The impact of altering chloride ion inlet concentration, set at 100, 300, and 500 mg/l, while keeping bed height (7 cm) and flow rate constant (5 ml/min), is depicted through the breakthrough curves as shown in Figure 7. It was observed that the adsorbent bed was exhausted earlier at higher concentrations. This rapid exhaustion of the bed is due to the swift saturation of binding sites within the column. Quicker exhaustion of the bed is unfavorable for optimal column performance (Radhika *et al.* 2018).

Therefore, striking a balance in choosing the operational concentration is crucial for achieving optimal column performance, considering both adsorption efficiency and breakthrough time. The initial concentration of chloride ions in the inlet flow is a critical factor affecting column performance. An increase in the inlet chloride ion concentration directs to a steeper slope of the breakthrough curve, resulting in a reduced volume treated before saturation of adsorbent bed.

Moreover, at a steady flow rate, an elevation in the inlet concentration of chloride ions reduces the throughput until reaching the breakthrough point. This phenomenon is ascribed to the rapid saturation of adsorbent sites by high chloride ion concentrations, thereby shortening the breakthrough time (Hussein & Mayer 2022).

The propagated uncertainty in the experimental data demonstrates the accuracy of adsorption capacity predictions (Badalyan & Pendleton 2003). For instance, it was discovered that the adsorption capacity (q_e) under standard experimental conditions was 85.441 $\pm$ 13 mg/g. When assessing the predictive models' goodness of fit, this degree of uncertainty was taken into consideration. This emphasizes the necessity of precise measurement and thorough error analysis in investigations involving adsorption.

In summary, the data signifies that the initial concentration of adsorbate ions significantly influences the breakthrough curve and column performance, emphasizing the importance of carefully selecting the operating concentration to achieve optimal removal efficiency and breakthrough time. In real water treatment scenarios, to increase the effectiveness of the mechanism of adsorption, pretreatment procedures like dilution or the preliminary removal of other interfering ions may be necessary for waters with high initial contamination concentrations (Osman *et al.* 2023).

Table 2 represents different experimental conditions studied along with breakthrough curve parameters.

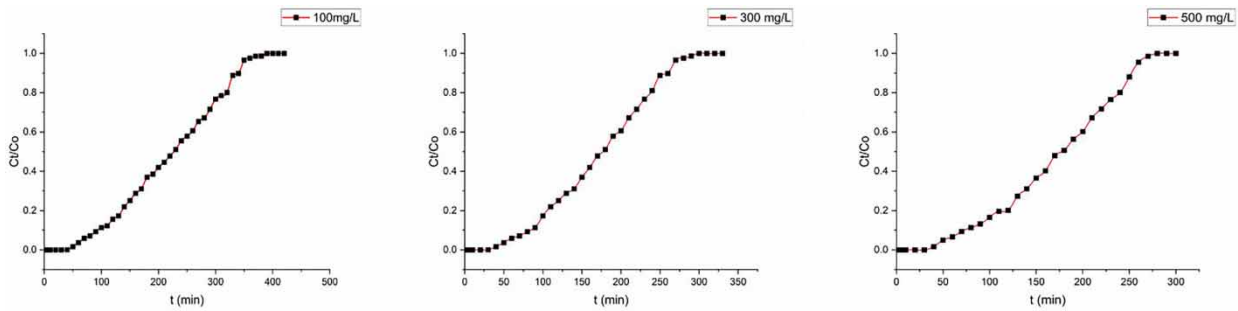

Figure 7 | Effect of a column-operating parameter – initial concentration on the breakthrough curve.

Table 2 | Different parameters for fixed-bed adsorption under different operating conditions

Experimental condition						V (ml)		
Bed height (cm)	**Flow rate (ml/min)**	**Initial concentration (mg/l)**	q_{total} (mg)	m_{total} (mg)	% Cl^- removed	V_b	V_T	q_e (mg/g)
5 ± 0.5	5 ± 0.5	500 ± 50	341.76 ± 54	625 ± 88	54.682 ± 11	200 ± 5	1,250 ± 5	85.441 ± 13
7 ± 0.5	5 ± 0.5	500 ± 50	429.76 ± 65	750 ± 106	57.302 ± 12	210 ± 5	1,500 ± 5	71.627 ± 11
10 ± 0.5	5 ± 0.5	500 ± 50	552.12 ± 81	950 ± 134	58.118 ± 12	250 ± 5	2,100 ± 5	69.015 ± 10
7 ± 0.5	3 ± 0.5	500 ± 50	421.335 ± 85	510 ± 99	82.615 ± 23	60 ± 5	1,020 ± 5	70.223 ± 14
7 ± 0.5	5 ± 0.5	500 ± 50	420 ± 64	750 ± 106	56 ± 11	50 ± 5	1,500 ± 5	70 ± 10
7 ± 0.5	7 ± 0.5	500 ± 50	419.468 ± 60	840 ± 103	49.93 ± 9	35 ± 5	1,680 ± 5	69.911 ± 10
7 ± 0.5	5 ± 0.5	100 ± 50	591.173 ± 302	1,000 ± 509	59.117 ± 42	200 ± 5	2,100 ± 5	98.529 ± 50
7 ± 0.5	5 ± 0.5	300 ± 50	484.175 ± 98	825 ± 160	58.688 ± 16	180 ± 5	1,650 ± 5	80.696 ± 16
7 ± 0.5	5 ± 0.5	500 ± 50	429.75 ± 65	750 ± 106	57.3 ± 11	150 ± 5	1,500 ± 5	71.625 ± 11

q_{total} = overall chloride ion adsorption capacity (mg), m_{total} = overall mass of adsorbed chloride ions (mg), V_b = volumetric output at breakthrough point (ml), V_T = total volumetric output at saturation (ml), q_e = adsorption capacity (mg/g).

Mathematical modeling of breakthrough curves

The data were fitted to the Thomas model to determine the values of both q_e (adsorption capacity, (mg/g)) and K_{Th} (rate constant, (ml/min/mg)) which were calculated from the intercept and slope of a plot of ln [Ct/Co] against t as shown in Table 1. The results for the dynamic modeling for column adsorption are shown in the Table 3. Accordingly, the study found that as the initial concentration of the adsorbate rose from 100 to 500 mg/l, the adsorption capacity (q_e) decreased, indicating a decline in accessible adsorption sites. In contrast, the Thomas constant (k) increased with initial concentration. Furthermore, increasing bed height improved adsorption capacity by adhering to increased adsorbent mass, whereas a decrease in the Thomas constant indicated slower kinetics owing to increased mass transfer resistance. This aligns with the assumptions drafted in the Thomas model stating and the rate of adsorption is directly proportional to the available adsorption sites (Mustafa & Ebrahim 2010). Notably, as the flow rate increased from 3 to 7 ml/min, adsorption capacity reduced, indicating decreased efficiency with higher flow rates, implying that higher flow rates decrease the duration of contact between the adsorbate and adsorbent, resulting in diminished adsorption capacity. Hence, it is possible to infer that as the flow rate rises, the driving force of mass transfer in the liquid film also increases (Tor *et al.* 2009). These findings emphasize the complex relationship between concentration gradients, mass transfer processes, and adsorption kinetics, providing important insights for optimizing chloride removal (Li *et al.* 2018).

In the Yoon–Nelson Model, it was found that the time needed to achieve 50% adsorbate breakthrough (τ) decreased with higher initial adsorbate concentrations, from 100 to 500 mg/l. Conversely, the Yoon–Nelson constant (K_{Y-N}) increased in proportion to the initial concentration. This can be attributed to faster saturation of adsorption sites leading to earlier breakthrough (Bakhta *et al.* 2024). Interestingly, raising the height of the adsorbent layer increased the breakthrough time, though not in direct proportion to the height (Ajmani *et al.* 2020). This phenomenon could be explained by a greater probability of preferential drainage channels developing when there is more adsorbent material present. It aligns with other findings that suggesting that the probability of an adsorbate breakthrough and the amount of adsorption capacity available determine the likelihood that adsorbate molecules will either be adsorbed or desorbed (Myers *et al.* 2023). Furthermore, increasing the flow rate from 3 to 7 ml/min resulted in increase in K_{Y-N}, whereas τ tends to decrease, indicating a slower breakthrough time. These findings align with similar observations reported in previous studies (Chowdhury *et al.* 2013).

The study also utilized the Clark model, which integrates mass transfer principles with the Freundlich isotherm to describe adsorption kinetics. Within this model, parameters A and r characterize the kinetic equation, with their values determined by the slope and intercept of the Clark model equation. The increase in A value as bed height rises shows that greater bed heights improve the adsorption capacity of the system (Yahya *et al.* 2020). Similarly, the increase in parameters A and r with higher flow rates indicates that higher flow rates enhance adsorption capacity, possibly due to increased mass transfer rates (Sun *et al.* 2014). However, the slight decrease in R^2 at the highest flow rate suggests that the model's accuracy may be impacted by rapid flow, possibly due to insufficient contact time between the adsorbate and adsorbent. Furthermore, the increase in A

Table 3 | Kinetic parameters obtained via non-linear regression

Effect of bed height variation

Thomas model						Yoon-Nelson model					Clark's model				
Height (cm)	q_e	K_{Th}	R^2	SSE	RMSE	K_{Y-N}	τ	R^2	SSE	RMSE	A	r	R^2	SSE	RMSE
5 cm	2.80	1.72	0.995	0.05	0.04	0.027	138.09	0.986	0.05	0.043	37.82	0.024	0.989	0.03	0.03
7 cm	94.75	0.03	0.998	0.03	0.03	0.024	175.01	0.99	0.03	0.034	51.91	0.020	0.996	0.01	0.02
10 cm	333.63	−0.007	0.996	0.09	0.04	0.017	254.33	0.982	0.09	0.046	58.05	0.014	0.994	0.04	0.03

Effect of flow rate variation

Thomas model						Yoon-Nelson model					Clark's model				
Flow Rate (ml/min)	q_e	K_{Th}	R^2	SSE	RMSE	K_{Y-N}	τ	R^2	SSE	RMSE	A	r	R^2	SSE	RMSE
3 ml/min	319.17	0.010	0.996	0.05	0.036	0.01	174.28	0.986	0.05	0.04	21.56	0.016	0.989	0.0722	0.04
5 ml/min	228.56	0.016	0.999	0.02	0.028	0.02	167.76	0.993	0.02	0.02	42.25	0.020	0.996	0.01	0.02
7 ml/min	203.71	0.010	0.997	0.03	0.037	0.03	129.80	0.989	0.03	0.03	48.31	0.026	0.990	0.03	0.03

Effect of initial concentration variation

Thomas model						Yoon-Nelson model					Clark's model				
Initial Concentration (mg/l)	q_e	K_{Th}	R^2	SSE	RMSE	K_{Y-N}	τ	R^2	SSE	RMSE	A	r	R^2	SSE	RMSE
100 mg/l	526.83	0.01	0.996	0.05	0.03	0.01	223.54	0.991	0.05	0.03	38.16	0.01	0.994	0.03	0.02
300 mg/l	200.54	0.01	0.996	0.02	0.02	0.02	174.06	0.994	0.02	0.02	51.59	0.02	0.996	0.02	0.02
500 mg/l	71.06	0.03	0.996	0.03	0.03	0.02	175.01	0.991	0.03	0.03	52.91	0.02	0.996	0.01	0.02

q_0 = Thomas Model adsorption capacity (mg/g), K_{Th} = Thomas constant (ml/mg/min), R^2 = correlation coefficient, K_{Y-N} = Yoon–Nelson Constant (min^{-1}), τ = time needed to achieve 50% adsorbate breakthrough (min), A & r = Clark's constants, SSE = sum of squares error, RMSE = root mean square error.

value with higher initial concentrations suggests that higher concentrations enhance adsorption capacity, likely due to a stronger driving force for mass transfer (Patel 2019). The consistent R^2 values across different concentrations demonstrate that the Clark model effectively captures adsorption behavior, even at high concentrations. This approach offers insights into the dynamics of chloride adsorption onto the activated vetiver root powder and provides a framework for understanding the underlying mechanisms driving the process (Długosz & Banach 2018).

Table 3 presents the column parameters obtained for the adsorption process under dynamic conditions using non-linear regressions. It is evident that all three models adequately captured the variation in the flow rate of adsorbate, initial concentration variation of adsorbate, and bed height.

The correlation coefficient values for all models using non-linear regression analysis were satisfactory, indicating their reliability in this study. Notably, the Thomas model exhibited adsorption capacity values (about 71.06 mg/g) across different variations close to the experimentally reported value (71.62 mg/g). Similar results have previously been reported by (Nwabanne *et al.* 2022). This also suggests that the non-linear regression analysis using the Thomas model may offer the most accurate description of the adsorption mechanism under dynamic conditions. Chosen error metrics, such as RMSE and SSE, were employed to evaluate the discrepancy between the experimental data and the model's non-linear predictions. Across all instances, the error metric values were below zero, suggesting minimal error dispersion in the model parameter predictions.

Computational modeling

As shown in Table 4, this investigation constructed a three-layer ANN model for assessing chloride ion biosorption employing activated vetiver powder in a continuous operating mode. A subset of the data was segregated comprising 70% for training,

Table 4 | ANN architecture

ANN architecture	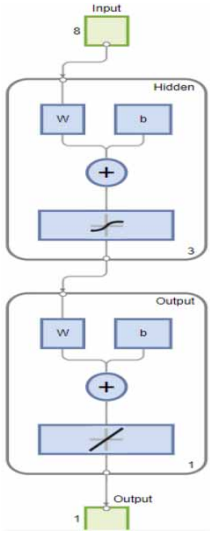
Input parameters	Bed height (cm), Flow rate (ml/min), Initial metal ions concentration (mg/l), qtotal (mg), mtotal (mg), % chloride removal (%), Volume of treated saline water at breakthrough point, V_b (ml) and volume of treated saline water at saturation point, V_T (ml), adsorption capacity (mg/g)
No. of layers	3
Training algorithm	Levenberg–Marquardt (trainlm)
Transfer function	Logsig
Max epochs	1,000
Training data, testing data	85%, 15%
RMSE	0.0405
R^2	0.99

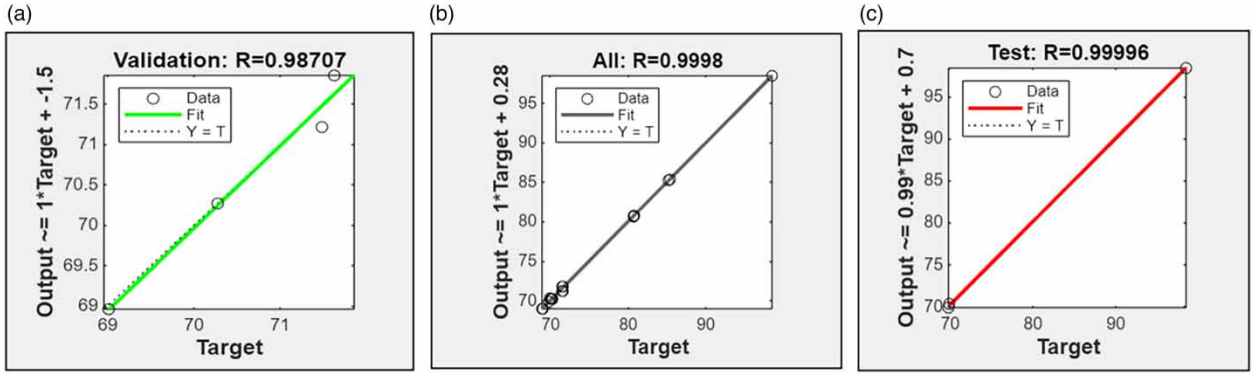

Figure 8 | Scatter plot for ANN indicating efficiency– (a) during training, (b) overall, and (c) during testing.

15% for validation and 15% for evaluating the predicted accuracy of the model (Nighojkar *et al.* 2022). Validation was performed to fine-tune the model and prevent overfitting. The testing subset provided an impartial evaluation of the performance of the model, while optimization of the model parameters was done using training data subset (Maleki *et al.* 2020). The ideal design was ascertained by training multiple feedforward networks to minimize mean squared error (MSE) (Chen *et al.* 2020). The chosen architecture for the ANN comprised a feedforward neural network with eight inputs, known as MLP (8:3:1:1), an output layer with one neuron, and a hidden layer with three neurons.

The constructed ANN model's correlation coefficient of 0.999 indicates its reliability (Figure 8(b)). Validation revealed that the model's overall prediction accuracy was 98% (Figure 8(a)). The model's accuracy in forecasting the removal of chloride ions was evaluated using data which was not used throughout the training phase; the results showed an R^2 value of 0.99 (Figure 8(c)).

CONCLUSION

The experimental results showed that activated vetiver root have promising ability to remove chloride ions from saline solutions. The study underscores the importance of bed height, flow rates, and initial concentration of adsorbate in chloride ion removal using activated vetiver root powder. Increased bed height enhances adsorption site availability and contact time, improving removal efficiency. Lower flow rates favor higher adsorption capacity, while rapid bed exhaustion at higher concentrations compromises performance. Balancing these factors is crucial for optimizing chloride removal in water treatment applications. Adsorption dynamic tests revealed that the breakthrough equations aligned closely with the experimental data, consistent with the principles of Thomas, Yoon–Nelson, and Clark. The non-linear equations of the models helped accurately determine the model parameters.

An excellent fit with the model's R^2 value of 0.999 and RMSE of 0.028 was obtained with the Thomas model, which postulates that the rate of adsorption is directly proportional to the number of empty sites. The Thomas model demonstrated that kinetic factors principally govern adsorption. The breakthrough time of the Yoon–Nelson model, which predicts precisely that 50% of the adsorbate chloride ions are eliminated, decreased as the initial concentration was raised. Yoon–Nelson showed a high R^2 value of 0.994 and an RMSE of 0.02. The Freundlich equilibrium isotherm and mass transfer principles are combined in the Clark model, which produced an R^2 value of 0.996 and an RMSE of 0.02. The adsorption capacity of the model is significantly influenced by parameter A, particularly at greater flow rates and higher bed heights. Sensitivity analysis of parameters indicated that variations in parameter A had a greater impact on the Clark model compared to parameter r. In the Yoon–Nelson model, variation in τ had more influence on the model than K_{Y-N}.

SEM analysis revealed that pores, fibers, hills, and pockets were the main components of the surfaces. Additionally, infrared and X-ray spectroscopies can deliver further insights into the adsorption mechanism by exploring the functional groups accountable for chloride ion uptake from saline solutions.

Precise forecasts for the elimination of chloride ions from saline solutions have been made possible using ANNs with R^2 value of 0.99 using the Levenberg–Marquardt algorithm. The approach can effectively anticipate the outcomes of bioadsorption, resulting in substantial savings of effort, time and expenses, as demonstrated by the accurate match between the predictions and the findings of the experiment.

Subsequent investigations should concentrate on examining the enduring stability and recyclable nature of powdered activated vetiver root in real-world water or wastewater treatment scenarios. Further research could examine the possibility of blending activated vetiver root powder with other nanomaterials or bioadsorbents to improve its selectivity and adsorption ability. Forecasting adsorption behavior under different circumstances by employing machine learning techniques could potentially be utilized for understanding the optimization of adsorption processes for upscaling or industrial applications.

ACKNOWLEDGEMENT

The authors extend their sincere gratitude to COEP Technological University Pune for their invaluable support and resources provided throughout this research endeavor.

AUTHOR CONTRIBUTIONS

R.C.D. and P.S. conceptualized the whole article and developed the methodology. R.C.D. performed the experimentation and presented the data for the first draft of the manuscript. P.S. provided guidance and reviewed the manuscript. All authors read and approved the final manuscript.

DATA AVAILABILITY STATEMENT

All relevant data are included in the paper or its Supplementary Information.

CONFLICT OF INTEREST

The authors declare there is no conflict.

REFERENCES

Abdiyev, K., Azat, S., Kuldeyev, E., Ybyraiymkul, D., Kabdrakhmanova, S., Berndtsson, R., Khalkhabai, B., Kabdrakhmanova, A. & Sultakhan, S. (2023) Review of slow sand filtration for Raw water treatment with potential application in less-Developed countries, *Water (Switzerland)*. https://doi.org/10.3390/w15112007.

Ahmad, A. A. & Hameed, B. H. (2010) Fixed-bed adsorption of reactive azo dye onto granular activated carbon prepared from waste, *J. Hazard Mater.*, **175**, 298–303. https://doi.org/10.1016/j.jhazmat.2009.10.003.

Ajmani, A., Patra, C., Subbiah, S. & Narayanasamy, S. (2020) Packed bed column studies of hexavalent chromium adsorption by zinc chloride activated carbon synthesized from Phanera vahlii fruit biomass, *J. Environ. Chem. Eng.*, **8**. https://doi.org/10.1016/j.jece.2020.103825.

Albadarin, A. B., Mangwandi, C., Al-Muhtaseb, H., Walker, G. M., Allen, S. J. & Ahmad, M. N. (2012) Modelling and fixed Bed column adsorption of Cr(VI) onto Orthophosphoric Acid-activated Lignin, *Chin. J. Chem. Eng.* **20** (3), 469–477.

Al-dhawi, B. N. S., Kutty, S. R. M., Jagaba, A. H., Aminu, N., Birniwa, A. H., Al-Shawesh, G. A. M. & Almahbashi, N. M. Y. (2024) Boron adsorption from aqueous solutions through column study: Desorption mechanisms, regeneration techniques, and kinetic insights, *Desalin. Water Treat*, **320**. https://doi.org/10.1016/j.dwt.2024.100586.

Altenor, S., Ncibi, M. C., Brehm, N., Emmanuel, E. & Gaspard, S. (2013) Pilot-scale synthesis of activated carbons from vetiver roots and sugar cane bagasse, *Waste Biomass Valorization*, **4**, 485–495. https://doi.org/10.1007/s12649-012-9180-0.

Badalyan, A. & Pendleton, P. (2003) Analysis of uncertainties in manometric gas-adsorption measurements. I: Propagation of uncertainties in BET analyses, *Langmuir*, **19**, 7919–7928. https://doi.org/10.1021/la020985t.

Bakhta, S., Sadaoui, Z., Bouazizi, N., Samir, B., Cosme, J., Allalou, O., Le Derf, F. & Vieillard, J. (2024) Successful removal of fluoride from aqueous environment using Al(OH)3@AC: Column studies and breakthrough curve modeling, *RSC Adv.*, **14**, 1–14. https://doi.org/10.1039/d3ra06697e.

Benjelloun, M., Miyah, Y., Akdemir Evrendilek, G., Zerrouq, F. & Lairini, S. (2021) Recent advances in adsorption kinetic models: Their application to Dye types, *Arab. J. Chem.*, https://doi.org/10.1016/j.arabjc.2021.103031.

Chen, Y., Song, L., Liu, Y., Yang, L. & Li, D. (2020) A review of the artificial neural network models for water quality prediction, *Appl. Sci. (Switzerland)*, https://doi.org/10.3390/app10175776.

Chowdhury, Z. Z., Zain, S. M., Rashid, A. K., Rafique, R. F. & Khalid, K. (2013) Breakthrough curve analysis for column dynamics sorption of Mn(II) ions from wastewater by using Mangostana garcinia peel-based granular-activated carbon, *J. Chem.*, https://doi.org/10.1155/2013/959761.

Chu, K. H. (2004) Improved fixed bed models for metal biosorption, *Chem. Eng. J.*, **97**, 233–239. https://doi.org/10.1016/S1385-8947(03)00214-6.

Darweesh, T. M. & Ahmed, M. J. (2017) Adsorption of ciprofloxacin and norfloxacin from aqueous solution onto granular activated carbon in fixed bed column, *Ecotoxicol. Environ. Saf.*, **138**, 139–145. https://doi.org/10.1016/j.ecoenv.2016.12.032.

Das, S. & Mishra, S. (2021) Artificial neural network (ANN) approach for prediction and modeling of breakthrough curve analysis of fixed-bed adsorption of iron ions from aqueous solution by activated carbon from Limonia acidissima shell, *Int. J. Chem. React. Eng.*, **19**, 1197–1219. https://doi.org/10.1515/ijcre-2021-0053.

Dey, S., Veerendra, G. T. N., Manoj, A. V. P. & Padavala, S. S. A. B. 2024 Removal of chlorides and hardness from contaminated water by using various biosorbents: A comprehensive review. *Water-Energy Nexus* **7**, 39–76. https://doi.org/https://doi.org/10.1016/j.wen.2024.01.003.

Dhumal, R. & Sadgir, P. (2023) Bioadsorbents for the removal of salt ions from saline water: A comprehensive review, *J. Eng. Appl. Sci.*, https://doi.org/10.1186/s44147-023-00253-1.

Dhumal, R. C. & Sadgir, P. (2024) Chloride ion sequestration by vetiver root biosorption: Isotherm, kinetic, and thermodynamic analyses and ANN prediction, *Water Supply.*, https://doi.org/10.2166/ws.2024.049.

Djelloul, C. & Hamdaoui, O. (2015) Dynamic adsorption of methylene blue by melon peel in fixed-bed columns, *Desalin. Water Treat*, **56**, 2966–2975. https://doi.org/10.1080/19443994.2014.963158.

Długosz, O. & Banach, M. (2018) Sorption of Ag+ and Cu2 + by vermiculite in a fixed-bed column: Design, process optimization and dynamics investigations, *Appl. Sci. (Switzerland)*, **8**. https://doi.org/10.3390/app8112221.

Fawzy, M., Nasr, M., Nagy, H. & Helmi, S. (2018) Artificial intelligence and regression analysis for Cd(II) ion biosorption from aqueous solution by Gossypium barbadense waste, *Environ. Sci. Pollut. Res.*, **25**, 5875–5888. https://doi.org/10.1007/s11356-017-0922-1.

Fierro, V., Torné-Fernández, V., Montané, D. & Celzard, A. (2008) Adsorption of phenol onto activated carbons having different textural and surface properties, *Microporous Mesoporous Mater.*, **111**, 276–284. https://doi.org/10.1016/j.micromeso.2007.08.002.

Han, R., Wang, Y., Zhao, X., Wang, Y., Xie, F., Cheng, J. & Tang, M. (2009) Adsorption of methylene blue by phoenix tree leaf powder in a fixed-bed column: Experiments and prediction of breakthrough curves, *DES*, **245**, 284–297. https://doi.org/10.1016/j.desal.200.

Harikumar, P. S., Jaseela, C. & Megha, T. (2010) Defluoridation of water using bioadsorbents, *Pollut. Res.*, **29**, 707–711. https://doi.org/10.4236/ns.2012.44035.

Hoek, E. M. V., Weigand, T. M. & Edalat, A. (2022) Reverse osmosis membrane biofouling: Causes, consequences and countermeasures, *NPJ Clean Water.*, https://doi.org/10.1038/s41545-022-00183-0.

Hu, Q., Liu, H., Zhang, Z. & Pei, X. (2020) Development of fractal-like clark model in a fixed-bed column, *Sep. Purif. Technol.*, **251**. https://doi.org/10.1016/j.seppur.2020.117396.

Hu, Q., Wang, D., Pang, S. & Xu, L. (2022) Prediction of breakthrough curves for multicomponent adsorption in a fixed-bed column using logistic and Gompertz functions, *A. J. Chem.*, **15**. https://doi.org/10.1016/j.arabjc.2022.104034.

Hussein, F. B. & Mayer, B. K. (2022) Fixed-bed column study of phosphate adsorption using immobilized phosphate-binding protein, *Chemosphere*, **295**. https://doi.org/10.1016/j.chemosphere.2022.133908.

Johnson, G. D., Sims, J. L. & Grove', J. H. (1989) Distribution of potassium and chloride in two soils as influenced by rate and time of kcl application and soil ph, *Tob. Sci.*, **33**, 35–39.

Karaivazoglou, N. A., Papakosta, D. K. & Divanidis, S. (2005) Effect of chloride in irrigation water and form of nitrogen fertilizer on Virginia (flue-cured) tobacco, *Field Crops Res.*, **92**, 61–74. https://doi.org/10.1016/j.fcr.2004.09.006.

Kaushal, S. S., Likens, G. E., Pace, M. L., Reimer, J. E., Maas, C. M., Galella, J. G., Utz, R. M., Duan, S., Kryger, J. R., Yaculak, A. M., Boger, W. L., Bailey, N. W., Haq, S., Wood, K. L., Wessel, B. M., Park, C. E., Collison, D. C., Aisin, B. Y. 'aaqob I., Gedeon, T. M., Chaudhary, S. K., Widmer, J., Blackwood, C. R., Bolster, C. M., Devilbiss, M. L., Garrison, D. L., Halevi, S., Kese, G. Q., Quach, E. K., Rogelio, C. M. P., Tan, M. L., Wald, H. J. S. & Woglo, S. A., 2021 Freshwater salinization syndrome: From emerging global problem to managing risks. *Biogeochemistry* **154**, 255–292. https://doi.org/10.1007/s10533-021-00784-w.

Khandanlou, R., Fard Masoumi, H. R., Ahmad, M. B., Shameli, K., Basri, M. & Kalantari, K. (2016) Enhancement of heavy metals sorption via nanocomposites of rice straw and Fe3O4 nanoparticles using artificial neural network (ANN), *Ecol. Eng.*, **91**, 249–256. https://doi.org/10.1016/j.ecoleng.2016.03.012.

Li, Y., Zhu, Y., Zhu, Z., Zhang, X., Wang, D. & Xie, L. (2018) Fixed-bed column adsorption of arsenic(V) by porous composite of magnetite/hematite/carbon with eucalyptus wood microstructure, *J. Environ. Eng. Landsc. Manag.*, **26**, 38–56. https://doi.org/10.3846/16486897.2017.1346513.

Maleki, F., Muthukrishnan, N., Ovens, K., Reinhold, C. & Forghani, R. (2020) Machine learning algorithm validation: From essentials to advanced applications and implications for regulatory certification and deployment, *Neuroimaging Clin. N. Am.*, https://doi.org/10.1016/j.nic.2020.08.004.

Mondal, M. K. (2009) Removal of Pb(II) ions from aqueous solution using activated tea waste: Adsorption on a fixed-bed column, *J. Environ. Manage.*, **90**, 3266–3271. https://doi.org/10.1016/j.jenvman.2009.05.025.

Mustafa, Y. A. & Ebrahim, S. E. (2010) Utilization of thomas model to predict the breakthrough curves for adsorption and ion exchange, *J. Eng.*

Myers, T. G., Cabrera-Codony, A. & Valverde, A. (2023) On the development of a consistent mathematical model for adsorption in a packed column (and why standard models fail), *Int. J. Heat. Mass. Transf.*, **202**. https://doi.org/10.1016/j.ijheatmasstransfer.2022.123660.

Nighojkar, A., Zimmermann, K., Ateia, M., Barbeau, B., Mohseni, M., Krishnamurthy, S., Dixit, F. & Kandasubramanian, B. (2022) Application of neural network in metal adsorption using biomaterials (BMs): A review†, *Environ. Sci. Adv.* **16** (4), 6206–6223. https://doi.org/10.1039/d2va00200k.

Nwabanne, J. T., Iheanacho, O. C., Obi, C. C. & Onu, C. E. (2022) Linear and nonlinear kinetics analysis and adsorption characteristics of packed bed column for phenol removal using rice husk-activated carbon, *Appl. Water Sci.*, **12**. https://doi.org/10.1007/s13201-022-01635-1.

Omitola, O. B., Abonyi, M. N., Akpomie, K. G. & Dawodu, F. A. (2022) Adams-Bohart, Yoon-Nelson, and Thomas modeling of the fix-bed continuous column adsorption of amoxicillin onto silver nanoparticle-maize leaf composite, *Appl. Water Sci.*, **12**. https://doi.org/10.1007/s13201-022-01624-4.

Osman, A. I., El-Monaem, E. M. A., Elgarahy, A. M., Aniagor, C. O., Hosny, M., Farghali, M., Rashad, E., Ejimofor, M. I., López-Maldonado, E. A., Ihara, I., Yap, P. S., Rooney, D. W. & Eltaweil, A. S. (2023) Methods to prepare biosorbents and magnetic sorbents for water treatment: A review, *Environ. Chem. Lett.*, https://doi.org/10.1007/s10311-023-01603-4.

Parsaei, M., Roudbari, E., Piri, F., El-Shafay, A. S., Su, C. H., Nguyen, H. C., Alashwal, M., Ghazali, S. & Algarni, M. (2022) Neural-based modeling adsorption capacity of metal organic framework materials with application in wastewater treatment, *Sci. Rep.*, **12**. https://doi.org/10.1038/s41598-022-08171-7.

Patel, H. (2019) Fixed-bed column adsorption study: A comprehensive review, *Appl. Water Sci.*, https://doi.org/10.1007/s13201-019-0927-7.

Radhika, R. T. J. G. R. K., Jayalatha, T., Jacob, S., Rajeev, R. & George, B. K. (2018) Adsorption performance of packed bed column for the removal of perchlorate using modified activated carbon, *Process Saf. Environ. Prot.*, **117**, 350–362. https://doi.org/10.1016/j.psep.2018.04.026.

Sharma, S. & Bhattacharya, A. (2017) Drinking water contamination and treatment techniques, *Appl. Water Sci.*, https://doi.org/10.1007/s13201-016-0455-7.

Sun, X. F., Imai, T., Sekine, M., Higuchi, T., Yamamoto, K., Kanno, A. & Nakazono, S. (2014) Adsorption of phosphate using calcined Mg3-Fe layered double hydroxides in a fixed-bed column study, *J. Ind. Eng. Chem.*, **20**, 3623–3630. https://doi.org/10.1016/j.jiec.2013.12.057.

Tor, A., Danaoglu, N., Arslan, G. & Cengeloglu, Y. (2009) Removal of fluoride from water by using granular red mud: Batch and column studies, *J. Hazard Mater.*, **164**, 271–278. https://doi.org/10.1016/j.jhazmat.2008.08.011.

Yahya, M. D., Muhammed, I. B., Obayomi, K. S., Olugbenga, A. G. & Abdullahi, U. B. (2020) Optimization of fixed bed column process for removal of Fe(II) and Pb(II) ions from thermal power plant effluent using NaoH-rice husk ash and Spirogyra, *Sci. Afr.*, **10**. https://doi.org/10.1016/j.sciaf.2020.e00649.

Yetilmezsoy, K. & Demirel, S. (2008) Artificial neural network (ANN) approach for modeling of Pb(II) adsorption from aqueous solution by Antep pistachio (Pistacia Vera L.) shells, *J. Hazard Mater.*, **153**, 1288–1300. https://doi.org/10.1016/j.jhazmat.2007.09.092.

Yusuf, M., Song, K. & Li, L. (2020) Fixed bed column and artificial neural network model to predict heavy metals adsorption dynamic on surfactant decorated graphene, *Colloids Surf. A. Physicochem. Eng. Asp.*, **585**. https://doi.org/10.1016/j.colsurfa.2019.124076.

First received 3 July 2024; accepted in revised form 11 September 2024. Available online 27 September 2024